In Situ Reaction Mechanism Studies on Ozone-Based Atomic Layer Deposition of Al_2O_3 and HfO_2

Martin Rose,[*,†] Jaakko Niinistö,[‡,§] Ingolf Endler,[†] Johann W. Bartha,[∥] Peter Kücher,[‡] and Mikko Ritala[§]

Fraunhofer IKTS, 01277 Dresden, Germany, Fraunhofer CNT, 01099 Dresden, Germany, Department of Chemistry, University of Helsinki, FI-00014 Helsinki, Finland, and Department of Electrical Engineering and Information Technology, IHM, Technische Universität Dresden, 01062 Dresden, Germany

LETTER

ABSTRACT The mechanisms of technologically important atomic layer deposition (ALD) processes, trimethylaluminium (TMA)/ozone and tetrakis(ethylmethylamino)hafnium (TEMAH)/ozone, for the growth of Al_2O_3 and HfO_2 thin films are studied in situ by a quadrupole mass spectrometer coupled with a 300 mm ALD reactor. In addition to released CH_4 and CO_2, water was detected as one of the reaction byproduct in the TMA/O_3 process. In the TEMAH/O_3 process, the surface after the ozone pulse consisted of chemisorpted active oxygen and −OH groups, leading to the release of H_2O, CO_2, and HNEtMe during the metal precursor pulse.

KEYWORDS: atomic layer deposition • quadrupole mass spectrometry • ozone • in situ • process monitoring • active oxygen

1. INTRODUCTION

Atomic layer deposition (ALD), based on sequential self-limiting surface reactions of applied precursors, has emerged as the method of choice to grow thin dielectric layers for microelectronic applications (1, 2). Among the most applied precursors in ALD are trimethylaluminium ($Al(CH_3)_3$, TMA) and tetrakis(ethylmethylamino)hafnium ($Hf(NEtMe)_4$, TEMAH) for the growth of Al_2O_3 and HfO_2, respectively. In both cases, the applied oxygen source has usually been water. However, for certain applications, e.g., in the deposition of high-permittivity (high-*k*) capacitor dielectrics in dynamic random access memories, the use of water is disadvantageous. Because of its large dipole momentum, water has a high surface affinity. Therefore, the purging of water is slow, which results in reduced throughput, especially in low-temperature deposition and when high-aspect-ratio structures are applied (1). In some recent applications, water was replaced by ozone as the oxygen source (2−6). Ozone can be purged more efficiently than water and does not require a special surface preparation (7). Therefore, ozone processes provide higher throughput and more flexibility.

To understand the chemistry behind ALD processes and to characterize reaction byproducts, it is important to analyze the actual growth mechanism in situ. A quadrupole mass spectrometer (QMS) coupled with the ALD chamber is an effective tool to study the surface reactions (8−11). However, in the case of ozone-based ALD processes the reaction mechanism studies, e.g., in situ QMS investigations have rarely been performed (12−15). The TMA/O_3 process for Al_2O_3 growth was recently studied by in situ QMS and Fourier transform infrared spectroscopy by Goldstein et al., who found CH_4 and CO_2 being released as the reaction byproduct (15). Somewhat unexpectedly, water was not detected. In the case of the TEMAH/O_3 process, the suggested main reaction byproducts were CO_2 and H_2O together with NO_x and CH_2O released during the combustive ozone pulse (11).

From a technological point of view, water is a very important species to be investigated as a reaction byproduct. Water generated during the growth process can have an effect on the growth mode and especially on conformality, e.g., in high-aspect -ratio structured wafers. If water is formed during the process and the purging between the precursors is inadequate, a chemical vapor deposition type growth mode can cause thickness nonuniformity. Additionally, in batch reactors, the surface area and therefore the amount of generated water can be extremely high, and thus the thickness uniformity can be seriously affected (16). Thus knowing the presence of water is essential in many cases.

An additional motivation of the current research was to study the suitability of QMS in ALD process metrology (17) in a DRAM capacitor dielectric production environment. ZrO_2−Al_2O_3−ZrO_2 (or HfO_2 instead of ZrO_2) capacitor dielectrics can achieve the specifications of the current technology node (18). In that laminate structure, a few ALD cycles of Al_2O_3 in between the ZrO_2 layers enables the required leakage current characteristics and thus it is of utmost importance that TMA/O_3 cycles have been deposited without problems.

* Corresponding author. E-mail: Martin.Rose@ikts.fraunhofer.de.
Received for review November 19, 2009 and accepted January 14, 2010
† Fraunhofer IKTS.
‡ Fraunhofer CNT.
§ University of Helsinki.
∥ Technische Universität Dresden.
DOI: 10.1021/am900807a
© 2010 American Chemical Society

2. EXPERIMENTAL SECTION

In the present letter, we have successfully coupled a QMS with an industrial scale 300 mm ALD reactor (FHR Anlagenbau GmbH) in order to investigate the reaction mechanisms of ozone-based Al_2O_3 and HfO_2 processes in situ. The reactor applied and the experimental setup have been described earlier (19). As the metal precursors, TMA (Air Liquide) and TEMAH (Air Liquide) were applied. Argon was used as a carrier and purging gas. Ozone (MKS Instruments, AX8560) in a concentration of 250 g/m^3 was used as the oxygen source. The applied substrate temperatures were 250 and 275 °C for both processes. The QMS experiments were performed using a MKS Microvision-IP. The mass spectrometer is differentially pumped and has two inlets. Inlet A was configured for a maximum pressure of 10 mbar, and inlet B was configured for a maximum pressure of 1×10^{-2} mbar. The electron energy was 40 eV at a current of 1 mA. Mass spectra were recorded at process pressures of 7 mbar using inlet A and 6×10^{-3} mbar using inlet B. When using the low pressure, the measured substrate temperature was 215 °C.

As substrates, 300 mm silicon wafers containing a high density of cylindrical trenches with an aspect ratio of 60:1 were used. The reactive surface area was about 2 m^2. The increased reactive surface area generates more byproduct during the surface reactions which results in a stronger QMS signal. Considering our standard reactor setup, the surface area of a planar 300 mm wafer (0.07 m^2) was not always sufficient to distinguish the signals originating from the byproducts and the background. These weak background signals are subtracted from the signals obtained during the actual ALD process, as described earlier (8). In addition, by comparative experiments, it was confirmed that the peaks obtained during the ALD process were originating from the heated substrate and not from the warm (150 °C) reactor walls. Thin films of the investigated materials were deposited on the substrate to a thickness of a few nanometers before the QMS experiments were conducted. The actual preconditioning takes place during the precursor background cycles. It should be noted that applying high-aspect-ratio trench wafer forced to lengthen the purge times in order to avoid overlapping of the precursor pulses. On the other hand, in microelectronic applications where ALD is applied, aspect ratios are often comparable to those used in this work so that valuable information can be obtained from this unique setup.

3. RESULTS AND DISCUSSION

The major byproducts of the TMA/O_3 process at 250 and 275 °C were CH_4 and CO_2. Methane (CH_4, $m/e = 16$) was released during both the TMA pulse and O_3 pulse as shown in Figure 1. CO_2 ($m/e = 44$) and its fragmentation product CO ($m/e = 28$) were detected only during the ozone pulse (data not shown). In contrast to the earlier study (15), water ($m/e = 18$) was clearly detected when the ozone pulse was longer than 3 s as shown in Figure 2. In this figure, A and C denote the background cycles of TMA and O_3, respectively. B denotes the full ALD cycles. The pulse sequence for each ozone pulse time is 3TMA + 3(TMA + O_3) + 3O_3. All peaks

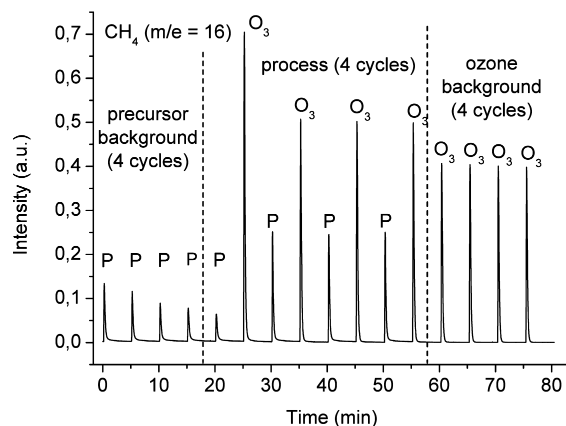

FIGURE 1. QMS signal of $m/e = 16$ during the TMA/O_3 process. Methane is released in both surface reactions. P and O_3 denote pulses of TMA and O_3, respectively.

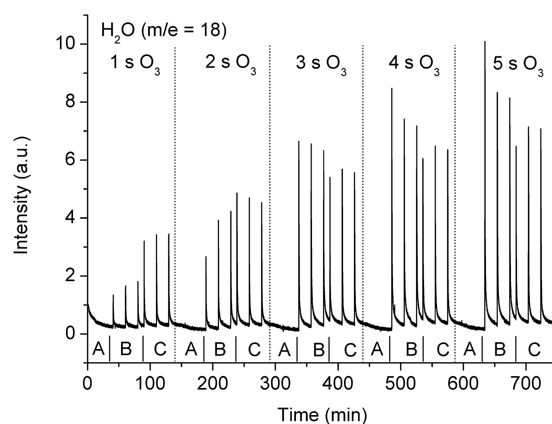

FIGURE 2. QMS signal of $m/e = 18$ during the TMA/O_3 process. A and C denote 3 repeated pulses of TMA and O_3, respectively. B denotes 3 complete ALD cycles. For 1 s ozone pulses, no water could be detected. Water was detected for ozone pulses longer than 3 s. All peaks occur during O_3 pulses.

in Figure 2 occurred during the ozone pulses. TMA chemisorbs to the surface releasing methane. The following ozone pulse partly combusts the remaining CH_3 ligands forming CO_2 and H_2O but also releases CH_4. This CH_4 is formed most likely by oxygen insertion into the Al−C bond (15). The formed H_2O is partly consumed by producing an −OH terminated surface. Ethylene ($m/e = 26-28$) and methanol ($m/e = 31$) were not detected. It is believed that, different from the previous study, in the present work, the detection of water was possible because both the reactive surface area and the ozone concentration were high. It should be noted that the intermediate surface species of formate and carbonate during the ozone pulse (oxygen insertion into the Al−C bond) can not be studied by QMS. Another reaction pathway suggested by Goldstein et al. (15), i.e., the oxygen insertion into the AlC-H bond seems less likely to have a major impact on the mechanism as ethylene was not detected. It should also be noted that the TMA/O_3 reaction mechanism is quite similar to the plasma-assisted ALD of Al_2O_3 from TMA/O_2 plasma, where combustion reactions due to oxygen radicals have been reported (20).

Knapas and Ritala showed a very interesting mechanism for the ZrO_2 ALD growth from $(CpMe)_2Zr(OMe)Me$ and O_3 (14). As expected, during the ozone pulse, CO_2 and H_2O were

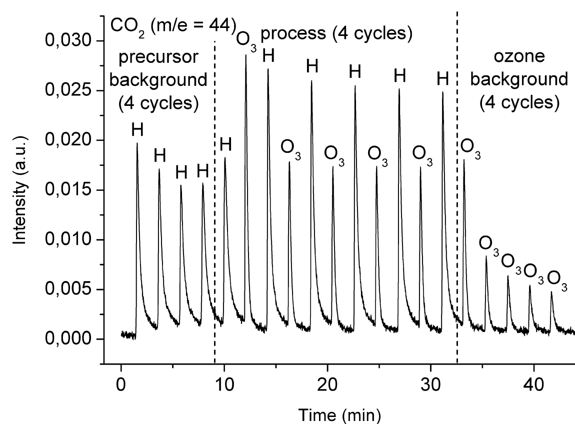

FIGURE 3. QMS signal of $m/e = 44$ during the TEMAH/O_3 process. CO_2 is released during both surface reactions. H and O_3 denote pulses of TEMAH and O_3, respectively.

released but also some active oxygen was chemisorbed on the surface reacting rapidly with the incoming Zr-precursor releasing CO_2 and H_2O again. Some of the H_2O formed −OH groups on the surface, which reacted with the −CpMe ligands. In the current TMA/O_3 process, no signs of the presence of active oxygen were detected, as no CO_2 and H_2O were detected during the TMA pulse.

However, the QMS reaction mechanism studies on the TEMAH/O_3 process at 275 °C showed clearly that the surface before the TEMAH pulse (after the ozone pulse) consists of OH groups and some chemisorbed active oxygen. The reaction byproducts released during the TEMAH pulse were HNEtMe ($m/e = 59$, data not shown), CO_2 as shown in Figure 3, and H_2O (data not shown). TEMAH reacts with the surface −OH groups releasing HNEtMe, as expected. The formation of CO_2 and H_2O, however, can be explained only by the presence of some active oxygen on the surface that reacts with the −NEtMe ligands. This finding gives further verification to the above-mentioned ZrO_2 study, where the formation of CO_2 and H_2O was observed during the precursor pulse (14). The data in the present or the previous study do not allow, however, identification of the chemical nature of active oxygen. In the simplest case, it can be just an oxygen atom (radical) bonded to surface cation (14).

During the ozone pulse the major byproducts were CO_2, H_2O, and NO_x (followed at $m/e = 30$, data not shown) in the current process. The mechanism here can be explained by ozone combusting the −NEtMe ligands. HNEtMe was not detected even when experiments were repeated at a very low pressure of 6×10^{-3} mbar, where the mean free path is considerably higher.

The deep trench substrates require rather long pulse times for saturation. Therefore the precursor and ozone pulse times were increased from 1 to 5 s, which clearly increased the amount of water generated as shown in Figure 4. It should be noted that the diffusion of water out from the deep trenches takes considerably long time so that purge times have to be sufficient in order to avoid pulse overlapping and CVD type growth. This has to be taken into account when optimizing film thickness uniformity.

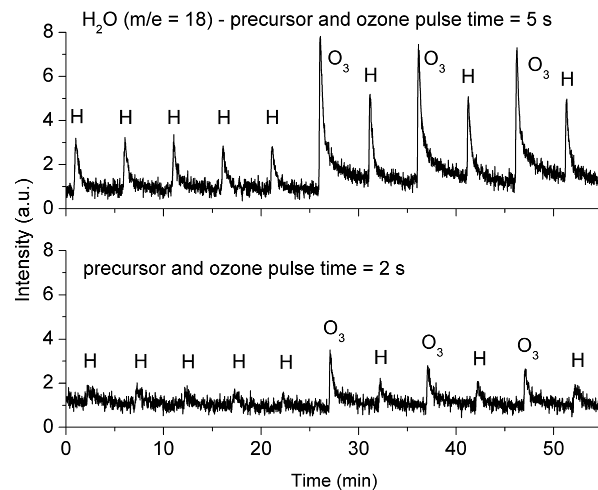

FIGURE 4. QMS signal of $m/e = 18$ during the TEMAH/O_3 process. Pulse times for the precursor and ozone were identical. The amount of detected water increases by 70% after the pulse times were extended to 5 s. H and O_3 denote pulses of TEMAH and O_3, respectively.

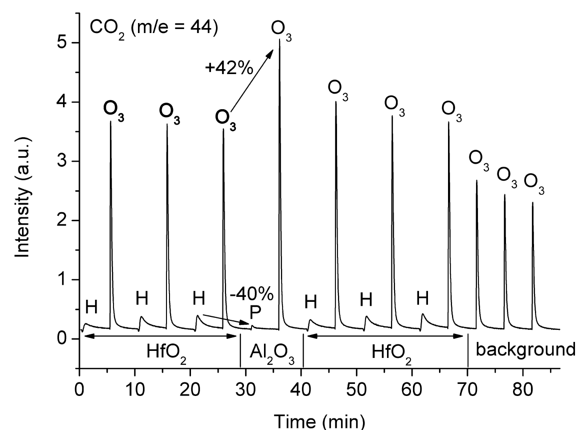

FIGURE 5. QMS signal of $m/e = 44$ during the deposition of HfO_2/Al_2O_3 laminates using TEMAH/TMA/O_3. H, P and O_3 denote pulses of TEMAH, TMA, and O_3, respectively.

Figure 5 shows an example of how a QMS coupled with an ALD reactor can be used to distinguish process cycles of different materials. The HfO_2 process releases different amounts of reaction byproduct than the Al_2O_3 process. Thus, for example one cycle of the TMA/O_3 process can be easily detected in the middle of the HfO_2 cycles and QMS can be used to monitor the process stability. The peak intensity of the CO_2 signal during the Al_2O_3 cycle is 42% higher than that during the HfO_2 cycle. Analogously, a decrease of the intensity was observed during the TMA pulses. The application of QMS in ALD production process metrology may be difficult, however, as the QMS should be coupled to the downstream of the exiting gases and the response times, at least for single wafer planar processes, may be too short to obtain clear signals.

4. CONCLUSIONS

We have shown a feasible way to characterize ALD reaction mechanisms of common ozone-based processes of Al_2O_3 and HfO_2 in an industrial scale reactor by in situ QMS. An important factor related to the TMA/O_3 process is the

LETTER

generation of H_2O as one of the reaction byproducts. The high substrate surface area enabled the increase of the QMS signal intensity. The presence of chemisorbed active oxygen left on the surface after the ozone pulse affected the TEMAH/O_3 reaction mechanism. Instead of releasing only HNEtMe during the metal precursor pulse, CO_2 and H_2O were also formed, meaning that the surface consists of −OH-groups and some chemisorbed active oxygen. This should be taken into account when the amount of water is of concern. The following ozone pulse combusts the organometallic ligands and H_2O and CO_2 are released again. Finally, an example of ALD process metrology for the growth of HfO_2−Al_2O_3−HfO_2 nanolaminates was shown.

Acknowledgment. This work was financially supported by the Sächsische Aufbaubank (Project 12458/2043) and the Academy of Finland (Project 128805).

REFERENCES AND NOTES

(1) Ritala, M.; Niinistö, J. In *Chemical Vapour Deposition: Precursors and Processes*; Jones, A. C., Hitchman, M. L., Eds.; Royal Society of Chemistry: Cambridge, U.K., 2009; pp 158−206.
(2) Niinistö, J.; Kukli, K.; Heikkilä, M.; Ritala, M.; Leskelä, M. *Adv. Eng. Mater.* **2009**, *11*, 223–234.
(3) Kim, S. K.; Choi, G. J.; Kim, J. H.; Hwang, C. S. *Chem. Mater.* **2008**, *20*, 3723–3727.
(4) Cho, H. J.; Kim, Y. D.; Park, D. S.; Lee, E.; Park, C. H.; Jang, J. S.; Lee, K. B.; Kim, H. W.; Ki, Y. J.; Han, I. K.; Song, Y. W. *Solid-State Electron.* **2007**, *51*, 1529–1533.
(5) Kosola, A.; Putkonen, M.; Johansson, L.-S.; Niinistö, L. *Appl. Surf. Sci.* **2003**, *211*, 102–112.
(6) Duenas, S.; Castan, H.; Garcia, H.; Gomez, A.; Bailon, L.; Kukli, K.; Niinistö, J.; Ritala, M.; Leskelä, M. *J. Vac. Sci. Technol., B* **2009**, *27*, 389–393.
(7) Kirsch, P. D.; Quevedo-Lopez, M. A.; Li, H.-J.; Senzaki, Y.; Peterson, J. J.; Song, S. C.; Krishnan, S. A.; Moumen, N.; Barnett, J.; Bersuker, G.; Hung, P. Y.; Lee, B. H.; Lafford, T.; Wang, Q.; Gay, D.; Ekerdt, J. G. *J. Appl. Phys.* **2006**, *99*, 023508.
(8) Rahtu, A.; Kukli, K.; Ritala, M. *Chem. Mater.* **2001**, *13*, 817–823.
(9) Matero, R.; Rahtu, A.; Ritala, M. *Langmuir* **2005**, *21*, 3498–3502.
(10) Henn-Lecordier, L.; Lei, W.; Anderle, M.; Rubloff, G. W. *J. Vac. Sci. Technol., B* **2007**, *25*, 130–139.
(11) Kim, M.-S.; Rogers, S. A.; Kim, Y.-S.; Lee, J.-H.; Kang, H.-K. *J. Korean Phys. Soc.* **2004**, *45*, 1317–1321.
(12) Liu, X.; Ramanathan, S.; Londergan, A.; Srivastava, A.; Lee, E.; Seidel, T. E.; Barton, J. T.; Pang, D.; Gordon, R. G. *J. Electrochem. Soc.* **2005**, *152*, G213–G219.
(13) Elam, J. W.; Martinson, A. B. F.; Pellin, M. J.; Hupp, J. T. *Chem. Mater.* **2006**, *18*, 3571–3578.
(14) Knapas, K.; Ritala, M. *Chem. Mater.* **2008**, *20*, 5698–5705.
(15) Goldstein, D. N.; McCormick, J. A.; George, S. M. *J. Phys. Chem. C* **2008**, *112*, 19530–19539.
(16) Granneman, E.; Fischer, P.; Pierreux, D.; Terhorst, H.; Zagwijn, P. *Surf. Coat. Technol.* **2007**, *201*, 8899–8907.
(17) Loo, J. P. *AIP Conf. Proc.* **2005**, *788*, 187–190.
(18) Cho, H. J.; Kim, Y. D.; Park, D. S.; Lee, E.; Park, C. H.; Jang, J. S.; Lee, K. B.; Kim, H. W.; Ki, Y. J.; Han, I. K.; Song, Y. W. *Solid-State Electron.* **2007**, *51*, 1529–1533.
(19) Rose, M.; Niinistö, J.; Michalowski, P.; Gerlich, L.; Wilde, L.; Endler, I.; Bartha, J. W. *J. Phys. Chem. C* **2009**, *113*, 21825–21830.
(20) Heil, S.; B, S.; Kudlacek, P.; Langereis, E.; Engeln, R.; van de Sanden, M. C. M.; Kessels, W. M. M. *Appl. Phys. Lett.* **2006**, *89*, 131505.

AM900807A